

Effect of thiourea, benzotriazole and 4,5-dithiaoctane-1,8-disulphonic acid on the kinetics of copper deposition from dilute acid sulphate solutions

E. E. FARNDON, F. C. WALSH, S. A. CAMPBELL*

Applied Electrochemistry Group, School of Chemistry, Physics & Radiography, University of Portsmouth, St. Michael's Building, White Swan Road, Portsmouth PO1 2DT, Great Britain

Received 13 April 1994; revised 26 October 1994

The effects of thiourea (TU), benzotriazole (BTA) and 4,5-dithiaoctane-1,8-disulphonic acid (DTODSA) on the deposition of copper from dilute acid sulphate solutions have been studied using potential sweep techniques. Tafel slopes and exchange current densities were determined in the presence and absence of these organic additives. TU and BTA were found to inhibit the copper deposition reaction; increases in the BTA concentration gave a systematic lowering of the exchange current density, whilst TU behaved in a less predictable manner. For BTA and TU concentrations of 10^{-5} mol dm⁻³, j_0 values of 0.0027 ± 0.0001 and 0.0028 ± 0.0002 mA cm⁻² were obtained compared to a value of 0.0083 ± 0.0003 mA cm⁻² for the additive free acid sulphate solution. In contrast, in the presence of DTODSA, an increased exchange current of 0.043 ± 0.0003 mA cm⁻² was observed. The presence of additives gave rise to measured Tafel slopes of -164 , -180 and -190 mV for TU, BTA and DTODSA, respectively, compared to that of -120 mV for copper sulphate alone.

List of symbols

A	electrode area (cm ²)	R	Molar gas constant (J K ⁻¹ mol ⁻¹)
b_C	cathodic Tafel slope (mV)	T	Temperature (K)
c_B	bulk concentration (mol cm ⁻³)	z	Number of electrons (dimensionless)
D	Diffusion coefficient (cm ² s ⁻¹)	<i>Greek symbols</i>	
F	Faraday constant (A s mol ⁻¹)	α_C	Cathodic transfer coefficient (dimensionless)
I_L	Limiting current (A)	η	Overpotential (V)
j	Current density (A cm ⁻²)	ν	Kinematic viscosity (cm ² s ⁻¹)
j_{CT}	Charge transfer current density (A cm ⁻²)	ω	Rotation rate (rad s ⁻¹)
j_0	Exchange current density (A cm ⁻²)		
k_L	Mass transport coefficient (cm s ⁻¹)		

1. Introduction

The scope for electrochemistry in the environment is extremely wide and spans many sectors of industry including the removal of metal ions from solution. Of particular importance is the removal of copper from aqueous liquors containing low levels of copper ions (1 to 100 mg dm⁻³) [1]. Such effluents are routinely produced by the electroplating industry in the form of spent or contaminated baths and rinsewaters [2]. These solutions contain not only the metal ion but also organics which have been added to the plating baths in order to produce the required surface finish, that is, substances acting as brighteners, levellers or wetting agents.

The presence of small amounts of these adsorption additives in the plating bath results in marked

changes in the deposit, which can include increased brightness, hardness, smoothness and ductility [3–5]. Examples of such additives include thiourea (TU), CS(NH₂)₂, benzotriazole (BTA), C₆H₅N₃, and 4,5-dithiaoctane-1,8-disulphonic acid (DTODSA), (HO₃SCH₂CH₂CH₂S⁻)₂. These addition agents have been shown to act as brighteners and levellers in acid plating baths and in their absence, dull copper deposits are formed. Surface roughness has been attributed to the fact that at high overpotentials mass transfer limited deposition favours the growth of a deposit with protrusions, whilst at low overpotentials the grain size of the deposit is large [6].

Whereas a great deal of work has been carried out on the kinetics of copper deposition and stripping from concentrated solutions (typically 0.1 to 0.5 mol dm⁻³) [7–13], very little kinetic data is available concerning deposition from low concentration copper solutions in the presence or absence of additives [14].

* Author to whom correspondence should be addressed.

This study is part of a programme to examine the effect of electrolyte additives on the kinetics of metal ion removal from dilute solutions. In particular, the effects of TU, BTA and DTODSA on the kinetics of copper deposition from dilute acidic copper sulphate solutions ($1 \times 10^{-3} \text{ mol dm}^{-3}$) have been investigated. Quantification of the kinetic parameters for the reaction aids the selection of appropriate conditions for the electrochemical treatment of copper contaminated industrial process solutions.

2. Experimental details

The reagents used were $\text{CuSO}_4 \cdot 5\text{H}_2\text{O}$ (Fluka puriss), Na_2SO_4 (BDH GPR), H_2SO_4 (Fisons AnalaR), TU (BDH), BTA (Aldrich Gold Label) and DTODSA (LeaRonol). All solutions were prepared with double distilled water and experiments were carried out at temperatures of $293 \pm 1 \text{ K}$. pH adjustments were made via the addition of sulphuric acid and were monitored on a Corning Model 150 pH meter with a BDH Gelplas combination pH electrode.

Electrochemical measurements were made using an EG&G 636 rotating disc electrode system coupled to a Sycopel 20V/2A potentiostat, a Hi-Tek PPR1 sweep generator and a Philips PM 8271 XYt chart recorder. The rotating disc electrode (RDE) consisted of a copper disc, 0.4 cm diam., set in an inert PTFE shroud of diam. 1.2 cm. The disc was polished using a $0.3 \mu\text{m}$ Al_2O_3 slurry. All experiments were carried out in a three compartment glass cell with the counter electrode compartment being separated from the working electrode using a NafionTM 423 cation exchange membrane. Electrode potentials were measured with respect to a saturated calomel electrode (SCE). Prior to each experiment, the cell was filled with electrolyte and purged with a fast stream of nitrogen for 15 min. The steady value of the rest potential of the copper working electrode was measured then the potential linearly swept to a value 800 mV more negative than this value. Polarization curves were obtained in this manner over a range of rotation rates from 250 rpm (26.2 rad s^{-1}) to 1750 rpm (183.3 rad s^{-1}) at a potential sweep rate of 10 mV s^{-1} . Tafel data were obtained at rotation rates of 1250 rpm (130.9 rad s^{-1}) and sweep rates of 1 mV s^{-1} . The rest potential of the working electrode, R_p was measured with respect to a SCE and the potential then swept to a value 650 mV more negative than this. Thick copper deposits which were difficult to remove, were produced on the electrode

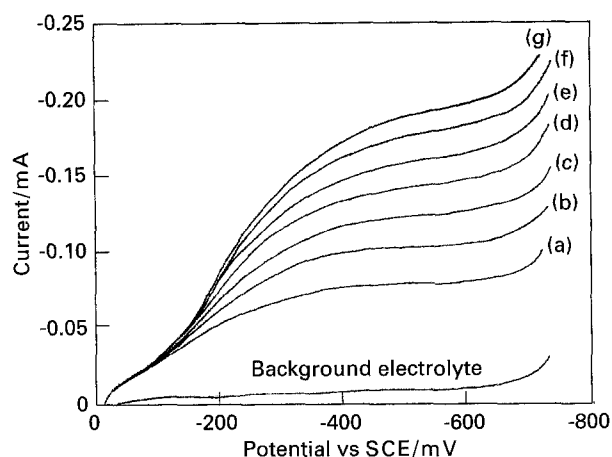


Fig. 1. Current-potential curves for the reduction of $1 \times 10^{-3} \text{ mol dm}^{-3} \text{ CuSO}_4$ in $0.5 \text{ mol dm}^{-3} \text{ Na}_2\text{SO}_4$ at pH 2.0 for rotation rates of (a) 250, (b) 500, (c) 750, (d) 1000, (e) 1250, (f) 1500 and (g) 1750 rpm. WE: copper disc, $r = 2 \text{ mm}$, RE: SCE and CE: Pt gauze. Potential sweep rate: 10 mV s^{-1} , $T = 293 \text{ K}$.

surface, if the potential was increased to more negative values.

3. Results and discussion

3.1. Additive-free copper solution

A series of polarization curves was obtained for a solution of $1 \times 10^{-3} \text{ mol dm}^{-3} \text{ CuSO}_4$ in $0.5 \text{ mol dm}^{-3} \text{ Na}_2\text{SO}_4$, adjusted to pH 2.0, in which the rotation rate was varied from 250 to 1750 rpm (26.2 to 183.3 rad s^{-1}) (Fig. 1). From these data, the diffusion coefficient for cupric ions at a rotating disc electrode (RDE) in a laminar flow regime, under steady state conditions, was calculated via the Levich equation [15]:

$$I_L = 0.62 n F A D^{2/3} \nu^{-1/6} \omega^{1/2} c_B \quad (1)$$

Linear plots of limiting current against square root of rotation rate were obtained, showing the copper deposition reaction to be mass transport controlled (see Fig. 2). The diffusion coefficient was $6.8 \pm 0.3 \times 10^{-6} \text{ cm}^2 \text{ s}^{-1}$ at 25° C , which is in good agreement with the literature values shown in Table 1 [14, 16–19].

Charge transfer data can be used in the characterization of the kinetics of the copper deposition reaction. Tafel plots showed a small charge transfer region, generally restricted to an overpotential range of -50 to -80 mV . At more negative potentials the charge transfer region was followed by one of mixed control where components of both charge transfer

Table 1. Diffusion coefficients for cupric ions in acid sulphate media $T = 298 \text{ K}$ [14, 16–19]

$[\text{Cu}^{2+}]$ $/10^{-3} \text{ mol dm}^{-3}$	Background electrolyte	$D/10^{-6} \text{ cm}^2 \text{ s}^{-1}$	Ref.
1.0	$0.5 \text{ mol dm}^{-3} \text{ Na}_2\text{SO}_4$ at pH 2.0	4.8	14
11	$0.7 \text{ mol dm}^{-3} \text{ H}_2\text{SO}_4$	5.8	16
40	$0.5 \text{ mol dm}^{-3} \text{ H}_2\text{SO}_4$	6.0	17
40	$0.5 \text{ mol dm}^{-3} \text{ Na}_2\text{SO}_4$ at pH 2.0	5.5	18
10	$0.1 \text{ mol dm}^{-3} \text{ Na}_2\text{SO}_4$ at pH 2.0	6.9	19

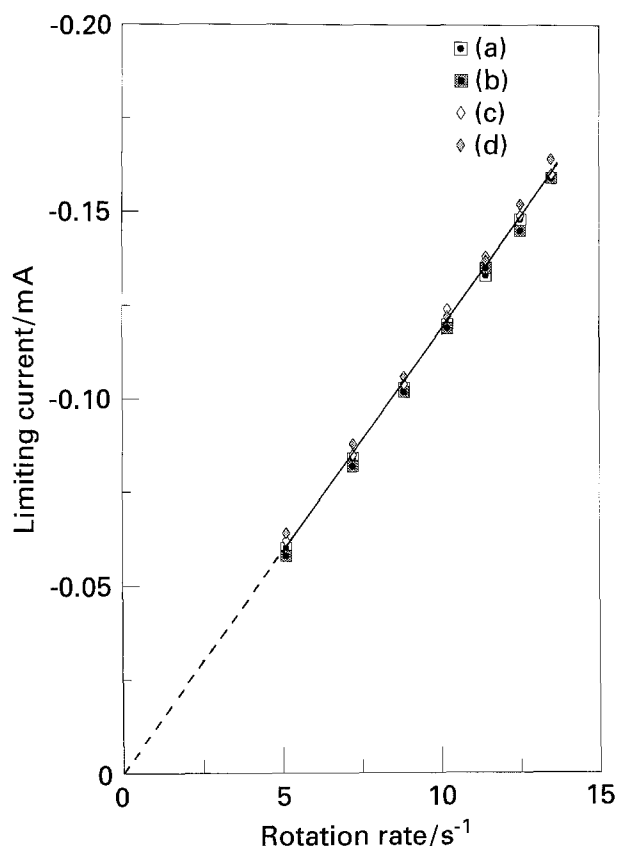


Fig. 2. Levich plots for $1 \times 10^{-3} \text{ mol dm}^{-3} \text{ CuSO}_4$ in Na_2SO_4 at pH 2.0 in the presence of (a) 0 mol dm^{-3} additive, (b) $1 \times 10^{-5} \text{ mol dm}^{-3}$ TU, (c) $1 \times 10^{-5} \text{ mol dm}^{-3}$ BTA and (d) $1 \times 10^{-5} \text{ mol dm}^{-3}$ DTODSA, $T = 293 \text{ K}$.

and mass transport contribute to the overall current. Studies of $0.3 \text{ mol dm}^{-3} \text{ CuSO}_4$ in $2.2 \text{ mol dm}^{-3} \text{ H}_2\text{SO}_4$ by Healy *et al.* [20] showed a similarly short Tafel region. However, a purely charge transfer controlled current density, j_{CT} , can be calculated from the total current density, j , via the expression,

$$\frac{1}{j} = \frac{1}{j_{\text{CT}}} + \frac{1}{j_{\text{L}}} \quad (2)$$

where j_{L} is the mass transport controlled limiting current density, as measured from the plateau region of the current-potential curves. The exchange current density, j_0 , and charge transfer coefficient α_{C} , can be determined from a plot of j_{CT} against overpotential, η , using the Tafel equation:

$$\log -j_{\text{CT}} = \log j_0 - \frac{\alpha_{\text{C}} n F}{2.3 RT} \eta \quad (3)$$

Figure 3 shows that a well defined linear region is obtained by plotting $\log j_{\text{CT}}$ against overpotential. The Tafel slope for 1×10^{-3} to $5 \times 10^{-2} \text{ mol dm}^{-3} \text{ CuSO}_4$ in the additive free solution at a rotation rate of 1250 rpm was found to be $-120 \pm 3 \text{ mV}$ and the corresponding charge transfer coefficient was 0.50. These values compared well with the Tafel slope of -120 mV and the charge transfer coefficient of 0.50 obtained by Mattsson and Bockris [7] for the deposition of copper from $1.0 \text{ mol dm}^{-3} \text{ CuSO}_4$ in $0.5 \text{ mol dm}^{-3} \text{ H}_2\text{SO}_4$ at $30 \pm 1^\circ \text{C}$. They showed that a charge transfer coefficient of 0.50 corresponded to

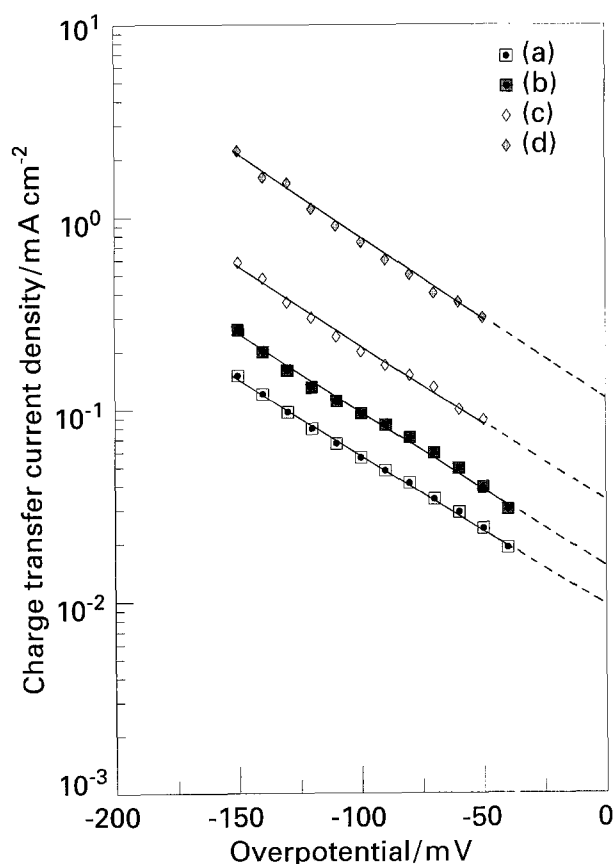
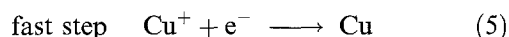
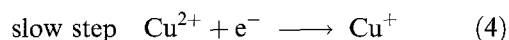
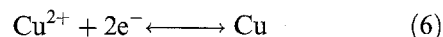


Fig. 3. Tafel extrapolations for (a) $1 \times 10^{-3} \text{ mol dm}^{-3}$, (b) $5 \times 10^{-3} \text{ mol dm}^{-3}$, (c) $10 \times 10^{-3} \text{ mol dm}^{-3}$ and (d) $50 \times 10^{-3} \text{ mol dm}^{-3} \text{ CuSO}_4$ in $0.5 \text{ mol dm}^{-3} \text{ Na}_2\text{SO}_4$ at pH 2.0. WE: Cu RDE, $r = 2 \text{ mm}$, rotation rate = 1250 rpm. CE: Pt gauze and RE: SCE. Potential sweep rate: 1 mV s^{-1} , $T = 293 \text{ K}$.

a classical two-stage mechanism for the deposition of copper:



It was proposed that the first step in this process occurred slowly and was rate controlling with Cu^+ existing in equilibrium with copper at the electrode surface. These results have subsequently been confirmed by many other workers [8, 9, 13]. However, others, including Hurlen [21], disagreed with this two step mechanism as they observed symmetrical anodic and cathodic Tafel slopes suggesting a single reduction process [21]:



In the present study, the exchange current density for the copper deposition reaction was found to increase with increasing cupric ion concentration from $0.0085 \pm 0.0003 \text{ mA cm}^{-2}$ for $1 \times 10^{-3} \text{ mol dm}^{-3}$ to $0.12 \pm 0.02 \text{ mA cm}^{-2}$ for $5 \times 10^{-2} \text{ mol dm}^{-3} \text{ CuSO}_4$. This trend is in agreement with the values obtained by Milora *et al.* [22] for higher concentration copper solutions, where j_0 values of 1.09 and 2.49 mA cm^{-2} were obtained for 0.1 and $1.0 \text{ mol dm}^{-3} \text{ CuSO}_4$ solutions, respectively. As expected, the heterogeneous rate constant for the electrodeposition reaction

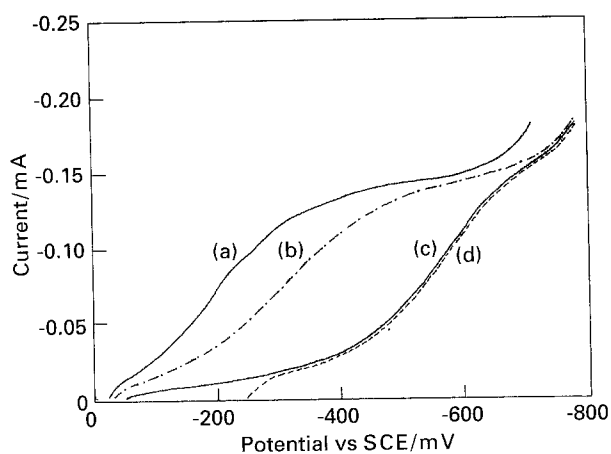


Fig. 4. Current-potential curves for the reduction of $1 \times 10^{-3} \text{ mol dm}^{-3} \text{ CuSO}_4$ in the presence of (a) 0 mol dm^{-3} , (b) $1 \times 10^{-6} \text{ mol dm}^{-3}$, (c) $1 \times 10^{-5} \text{ mol dm}^{-3}$ or $1 \times 10^{-4} \text{ mol}^{-3}$ and (d) $1 \times 10^{-3} \text{ mol dm}^{-3}$ TU. WE: Cu RDE, $r = 2 \text{ mm}$, rotation rate: 1250 rpm, RE: SCE and CE: Pt gauze. Potential sweep rate: 10 mV s^{-1} , $T = 293 \text{ K}$.

decreases for more dilute solutions, that is, the reaction kinetics become slower.

3.2. Copper deposition in the presence of thiourea

Polarization curves for 5×10^{-6} to $1 \times 10^{-3} \text{ mol dm}^{-3}$ TU in $1 \times 10^{-3} \text{ mol dm}^{-3} \text{ CuSO}_4$ are shown in Fig. 4. There is a decrease in the open circuit potential from -56 to -236 mV as the TU concentration increases from 5×10^{-6} to $1 \times 10^{-3} \text{ mol dm}^{-3}$. This is in contrast with more concentrated copper solutions, where the addition of small amounts of TU to the copper solutions causes the open circuit potential to become more positive and only at higher concentrations does the potential shift to more negative values [4]. However, the open circuit potential at a given additive concentration was not affected by rotation rate and the onset of hydrogen evolution occurred at -850 mV compared to a value of -700 mV for the additive free copper solution. Also, the limiting

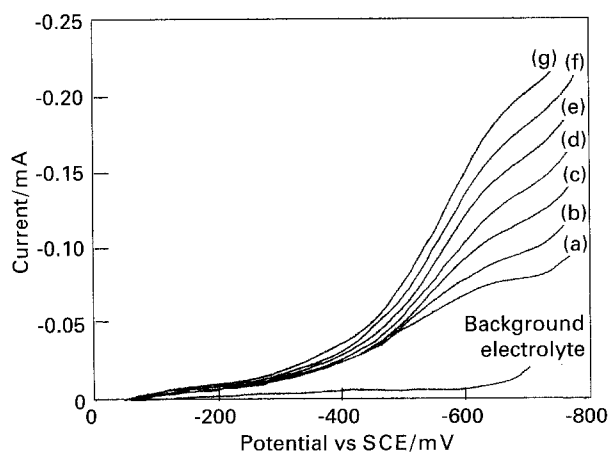


Fig. 5. Current-potential curves for the reduction of $1 \times 10^{-3} \text{ mol dm}^{-3} \text{ CuSO}_4$ in $0.5 \text{ mol dm}^{-3} \text{ Na}_2\text{SO}_4$ at pH 2.0 in the presence of $1 \times 10^{-5} \text{ mol dm}^{-3}$ TU. Rotation rates of (a) 250, (b) 500, (c) 750, (d) 1000, (e) 1250, (f) 1500 and (g) 1750 rpm. WE: Cu RDE, $r = 2 \text{ mm}$, RE: SCE and CE: Pt gauze. Potential sweep rate: 10 mV s^{-1} , $T = 293 \text{ K}$.

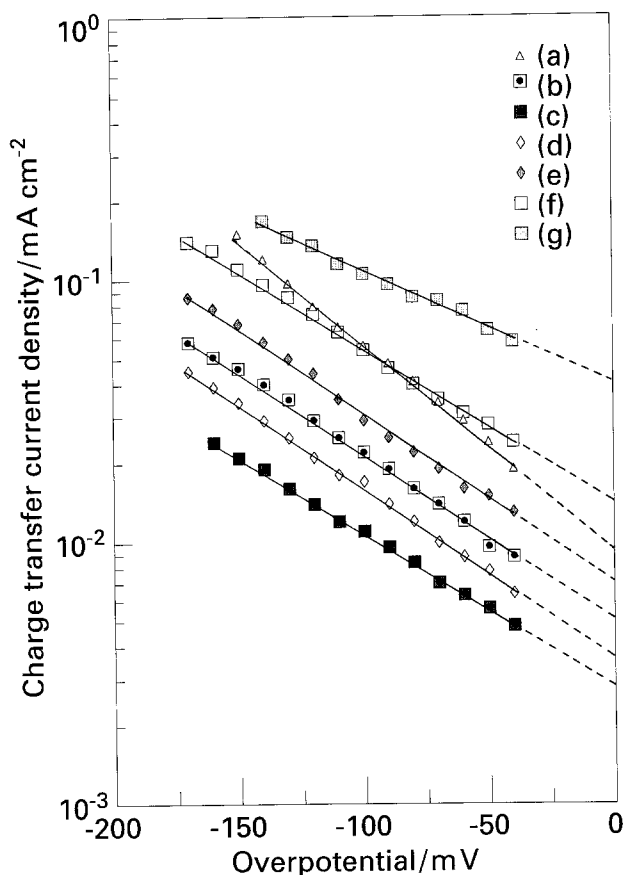


Fig. 6. Tafel extrapolations for $1 \times 10^{-3} \text{ mol dm}^{-3} \text{ CuSO}_4$ in $0.5 \text{ mol dm}^{-3} \text{ Na}_2\text{SO}_4$ at pH 2.0 in the presence of (a) 0, (b) 5×10^{-6} , (c) 1×10^{-5} , (d) 2×10^{-5} , (e) 5×10^{-5} , (f) 5×10^{-4} , (g) $1 \times 10^{-3} \text{ mol dm}^{-3}$ TU. WE: Cu RDE, $r = 2 \text{ mm}$, RE: SCE and CE: Pt gauze. Potential sweep rate: 1 mV s^{-1} , rotation rate: 1250 rpm, $T = 293 \text{ K}$.

plateau becomes less well defined with increasing amounts of additive (Fig. 5).

Figure 5 shows limiting current curves for $1 \times 10^{-3} \text{ mol dm}^{-3} \text{ CuSO}_4$ in the presence of $1 \times 10^{-5} \text{ mol dm}^{-3}$ TU. A diffusion coefficient of $6.8 \pm 0.3 \text{ cm}^2 \text{ s}^{-1}$ at 20° C was obtained, which remained constant for all concentrations of TU. The limiting current at -650 mV vs SCE was proportional to the square root of rotation rate and therefore, the copper deposition reaction can be said to be completely mass transport controlled.

Tafel kinetics for copper deposition from solutions containing TU showed marked changes compared with those for pure copper solutions. Figure 6 shows cathodic Tafel slopes for $1 \times 10^{-3} \text{ mol dm}^{-3} \text{ CuSO}_4$ in the presence of 0 to $1 \times 10^{-3} \text{ mol dm}^{-3}$ TU. An increase in the Tafel slope from its original value of $-120 \pm 3 \text{ mV}$ for the additive free solution to $-164 \pm 4 \text{ mV}$ for those containing 5×10^{-6} to $5 \times 10^{-4} \text{ mol dm}^{-3}$ TU was observed. The corresponding charge transfer coefficient, assuming a one electron change, was found to be 0.35. However, the Tafel slope increased to $-204 \pm 5 \text{ mV}$ with a corresponding decrease in the transfer coefficient to a value of 0.26 for higher concentrations of TU, $1 \times 10^{-3} \text{ mol dm}^{-3}$. This is in agreement with other studies on high concentration copper solutions

Table 2. Exchange current densities for $1 \times 10^{-3} \text{ mol dm}^{-3} \text{ CuSO}_4$ in $0.5 \text{ mol dm}^{-3} \text{ Na}_2\text{SO}_4$ at pH 2.0 in the presence of TU

Concentration of TU $/10^{-6} \text{ mol dm}^{-3}$	Exchange current density $/\text{mA cm}^{-2}$
0	0.0085 ± 0.0003
5	0.0048 ± 0.0006
10	0.0027 ± 0.0004
20	0.0036 ± 0.0002
50	0.0070 ± 0.0001
500	0.015 ± 0.0007
1000	0.040 ± 0.0001

WE: Cu disc, CE: Pt gauze, RE: SCE, $\omega = 1250 \text{ rpm}$ and $T = 293 \text{ K}$.

which also reported decreased transfer coefficients for increasing TU concentrations [4]. In this work a limiting value for the transfer coefficient of approximately 0.20 was obtained for a TU concentration of $10^{-4} \text{ mol dm}^{-3}$ in $1.0 \text{ mol dm}^{-3} \text{ CuSO}_4$. The observed changes in the cathodic Tafel slope and the corresponding decrease in α_C in the presence of TU, for both concentrated and dilute sulphate solutions, suggest that the process taking place on the electrode surface can no longer be a simple one electron transfer. This may be attributed to complex formation between TU and cuprous ions at the electrode surface.

The variation in exchange current density with TU concentration was more complex. At concentrations of 5×10^{-6} and $5 \times 10^{-5} \text{ mol dm}^{-3}$ TU, exchange current densities of 0.0048 ± 0.0006 and $0.0070 \pm 0.0001 \text{ mA cm}^{-2}$ were observed which are lower than that of $0.0085 \pm 0.0003 \text{ mA cm}^{-2}$ observed for the additive free copper solution. At higher concentrations of 5×10^{-4} and $1 \times 10^{-6} \text{ mol dm}^{-3}$ TU, exchange current densities of between 0.015 ± 0.0007 and $0.040 \pm 0.0002 \text{ mA cm}^{-2}$ were found. This variation in exchange current density with TU concentration was not systematic and a linear relationship between concentration and j_0 was not observed (see Table 2). Milora *et al.* [22] found a similar relationship between exchange current density and TU concentration for more concentrated copper sulphate solutions.

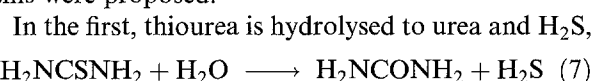
The observed decreases in the exchange current density in the presence of TU suggest that it must be acting as an inhibitor which is confirmed by the observation that at any given overpotential the current density for copper deposition from solutions up to and including $5 \times 10^{-5} \text{ mol dm}^{-3}$ TU is lower than that found for the corresponding additive free solutions. However, when the concentration of TU is further increased to 5×10^{-4} and $1 \times 10^{-3} \text{ mol dm}^{-3}$, the converse is true and the current increases at a given overpotential. Two very different concentration-dependent effects are operative and these can be related to the different complexes possible as discussed below.

3.3. Mechanisms for the action of thiourea

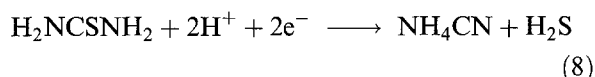
Several theories have been put forward to explain the

interactions between TU and the electrodeposition of copper from acid plating baths all of which involve adsorption of the additive at the electrode surface [3, 4]. Two main mechanisms have been suggested. In the first, 'structure-sensitive' adsorption of the additive occurs, with only molecules of a certain size, shape, and chemical structure adsorbed at the metal surface. The second mechanism involves 'current density' or 'shape sensitivity' where the additive is adsorbed at areas of high current density slowing down the rate of growth in this area and allowing more rapid growth in regions of low current density, thus producing a smooth surface.

Turner *et al.* [4] showed, via radiotracer methods, that the copper deposit contained a small amount of CuS which lead to the assumption that the TU decomposed during electrolysis and two possible mechanisms were proposed:



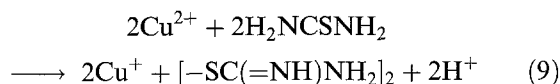
In the second, thiourea is reduced to form NH_4CN and H_2S ,



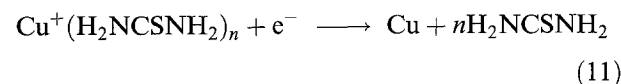
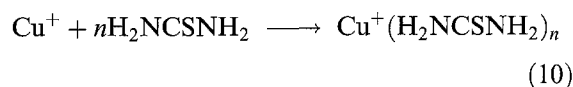
The authors believed the latter mechanism to be more likely, although no proof was offered. Whatever the actual mechanism, the H_2S thus produced reacts with the copper to produce the sulphide. The solubility product of CuS is low and, therefore, in the presence of low concentrations of sulphide ions, it will be precipitated at the cathode surface. This precipitate can interfere with normal crystal growth and may even block growth sites and increase the number of nucleation sites. This is consistent with the fact that copper deposited from solutions containing TU has a large number of small grains [3].

A second theory due to Zukauskaitė *et al.* [23] considered reactions in the electrolyte phase and at the cathode surface:

In solution



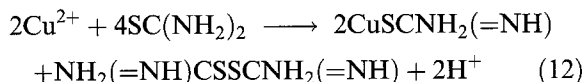
At the cathode



where $n = 1, 4$ or 6 [24, 25].

They suggested that Cu^+ forms an adsorbed complex with TU at low current densities whereas at high current densities saturation is attained, with respect to TU, and Cu^{2+} may discharge from the aquo complex. Over the range of potentials used during the electrodeposition of copper, it is thermodynamically possible to cathodically reduce formamidine

disulphide to TU. However, reduction of Cu^{2+} by TU is possible only when stable complexes are formed with Cu^+ and when the complex formation constant of these complexes is substantially higher than the corresponding constant for Cu^{2+} . When there is a considerable excess of Cu^{2+} with respect to TU it is most likely that 1:1 complexes form as shown below:



There are several possible alternatives for the structure of the complex $\text{Cu}^+(\text{SC}(\text{NH}_2)_2)_n$, where $n = 1, 4$ or 6 . For example, when $n = 6$, the compound could be $[\text{Cu}_4(\text{SC}(\text{NH}_2)_2)_6]^{4+}$, the structure of which is a tetrahedral or distorted Cu_4 core. In complexes with a Cu_4 tetrahedron, the atoms are bridged by S to give a Cu_4S_6 core, the structure is linked with six membered CuSCuSCuS rings [24]. If $n = 1$ or 4 , there is evidence of $[\text{Cu}_2\text{SC}(\text{NH}_2)_2]^{2+}$ or $[\text{Cu}(\text{SC}(\text{NH}_2)_2)_4]^+$ [25].

According to the above theories, at low concentrations, the complex produced at the electrode surface would be $\text{CuSCNH}_2(=\text{NH})$, whereas for the more concentrated solutions the reaction shown in Equation 10 offers the most likely mechanism.

3.4. Copper deposition in the presence of benzotriazole

Polarization curves were obtained for 5×10^{-6} to $1 \times 10^{-4} \text{ mol dm}^{-3}$ BTA in $1 \times 10^{-3} \text{ mol dm}^{-3}$ CuSO_4 and are shown in Fig. 7. The open circuit potential becomes more negative with increasing additive concentration, the value increasing from -46 mV in the absence of the additive to -85 mV with $1 \times 10^{-4} \text{ mol dm}^{-3}$ BTA. As in the case of TU, there was no change in these values when the rotation rate was altered and the limiting current plateau for BTA was shorter than that of the additive free copper solution. At BTA concentrations of $1 \times 10^{-4} \text{ mol dm}^{-3}$ no limiting current plateau is observed and the copper deposition reaction occurs in the region of hydrogen

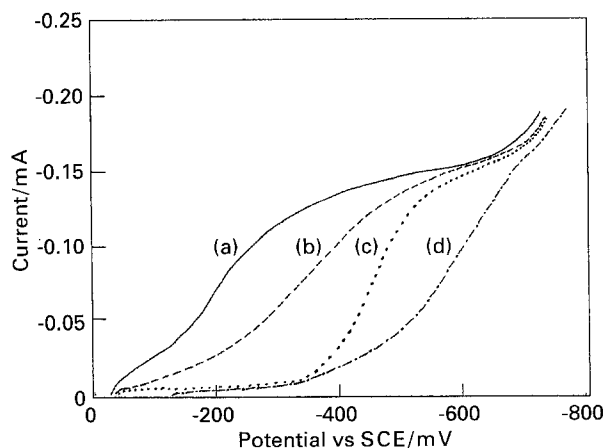


Fig. 7. Current-potential curves for the reduction of $1 \times 10^{-3} \text{ mol dm}^{-3}$ CuSO_4 in the presence of (a) 0, (b) 1×10^{-6} , (c) 1×10^{-5} and (d) $1 \times 10^{-4} \text{ mol dm}^{-3}$ BTA. WE: Cu RDE, $r = 2 \text{ mm}$, rotation rate: 1250 rpm , RE: SCE and CE: Pt gauze. Potential sweep rate: 10 mV s^{-1} , $T = 293 \text{ K}$.

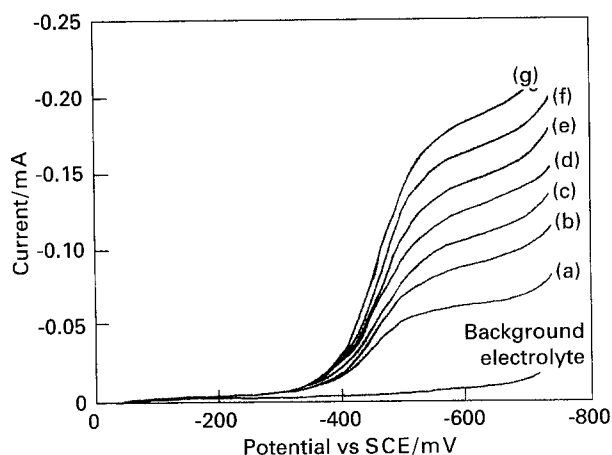


Fig. 8. Current-potential curves for the reduction of $1 \times 10^{-3} \text{ mol dm}^{-3}$ CuSO_4 in 0.5 mol dm^{-3} Na_2SO_4 at pH 2.0 in the presence of $1 \times 10^{-5} \text{ mol dm}^{-3}$ BTA. Rotation rates of (a) 250, (b) 500, (c) 750, (d) 1000, (e) 1250, (f) 1500 and (g) 1750 rpm. WE: Cu RDE, $r = 2 \text{ mm}$, RE: SCE and CE: Pt gauze. Potential sweep rate: 10 mV s^{-1} , $T = 293 \text{ K}$.

evolution, but concentration decay studies show that copper deposition is still occurring at potentials of -650 mV [26].

Figure 8 shows the limiting current curves obtained for $1 \times 10^{-3} \text{ mol dm}^{-3}$ CuSO_4 in the presence of $1 \times 10^{-5} \text{ mol dm}^{-3}$ BTA. The diffusion coefficient for the $\text{Cu}(\text{II})$ ion, calculated from Levich plots, Fig. 2, was $7.2 \pm 0.4 \text{ cm}^2 \text{ s}^{-1}$. Additive concentrations of 5×10^{-6} to $1 \times 10^{-5} \text{ mol dm}^{-3}$ did not alter this value and as the Levich equation is obeyed the copper deposition process is mass transport controlled.

Similarly to TU, the charge transfer data for copper solutions containing BTA showed differences to additive free copper solution (Fig. 9). Tafel slopes of $-180 \pm 2 \text{ mV}$ were obtained for copper in the presence of 5×10^{-6} to $5 \times 10^{-5} \text{ mol dm}^{-3}$ BTA and the corresponding charge transfer coefficient, assuming a one electron change, was 0.32, indicative of a more complex electrode process. These results compared well with those obtained by Shedshadri [27] who obtained Tafel slopes of -180 mV for 0.25 mol dm^{-3} CuSO_4 in 0.1 mol dm^{-3} H_2SO_4 with BTA concentrations of between $1 \times 10^{-6} \text{ mol dm}^{-3}$ and $1 \times 10^{-5} \text{ mol dm}^{-3}$.

The exchange current density decreased systematically with increasing BTA concentration from $0.0035 \pm 0.0003 \text{ mA cm}^{-2}$ at $5 \times 10^{-6} \text{ mol dm}^{-3}$ BTA to $0.00078 \pm 0.00001 \text{ mA cm}^{-2}$ at $1 \times 10^{-4} \text{ mol dm}^{-3}$ BTA. These j_0 values were considerably lower than those obtained in the additive free solution or in solutions containing TU. This, together with the decrease in current density at a given overpotential, showed that the deposition of copper is markedly inhibited in the presence of BTA.

3.5. Mechanism of action of benzotriazole

Shedshadri [27] attributed the increase in Tafel slope in the presence of BTA to the formation of a

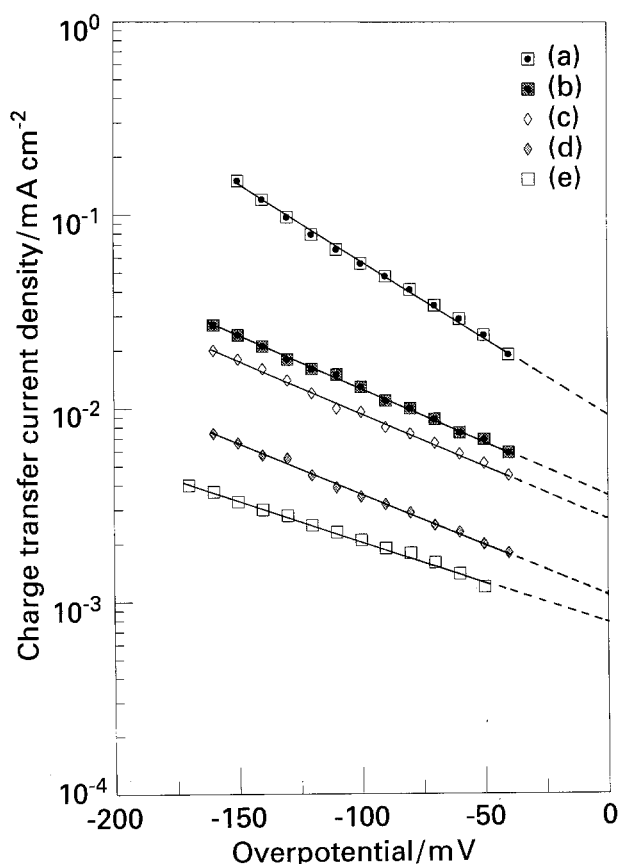
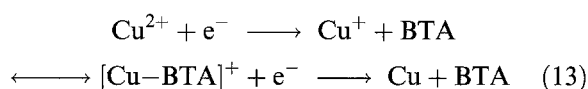


Fig. 9. Tafel extrapolations for $1 \times 10^{-3} \text{ mol dm}^{-3}$ CuSO_4 in 0.5 mol dm^{-3} Na_2SO_4 at pH 2.0 in the presence of (a) 0, (b) 5×10^{-6} , (c) 1×10^{-5} , (d) 5×10^{-5} and (e) $1 \times 10^{-4} \text{ mol dm}^{-3}$ BTA. WE: Cu RDE, $r = 2 \text{ mm}$, rotation rate: 1250 rpm, RE: SCE and CE: Pt gauze. Potential sweep rate: 1 mV s^{-1} , $T = 293 \text{ K}$.

copper–BTA complex.



Such complexes are known to form in neutral and acidic solution, where the BTA is chemisorbed forming a $[\text{Cu-BTA}]^+$ complex at the electrode surface [28, 29]. The inhibiting effect of the BTA on the copper deposition reaction may be due to the adsorption of the complex at active sites, where it may accept an electron from the cathode and discharge copper atoms which are incorporated at the active sites. The BTA which is released can then form a complex, a process which requires high energy and large overpotentials. Scanning tunnelling microscopy studies by Armstrong *et al.* [6] have shown a reduction in the particle size of the copper deposit on addition of BTA lead to increases in overpotential required to deposit the metal. Increased nucleation accounts for the change in the Tafel slope and the inhibiting effect of the additive.

Poling [30] investigated the structure and thickness of films formed on mirror copper surfaces in the presence of BTA using reflectance infrared spectroscopy. These studies showed that the N–H band observed with BTA disappeared when a CuBTA complex was formed, indicating that the copper was

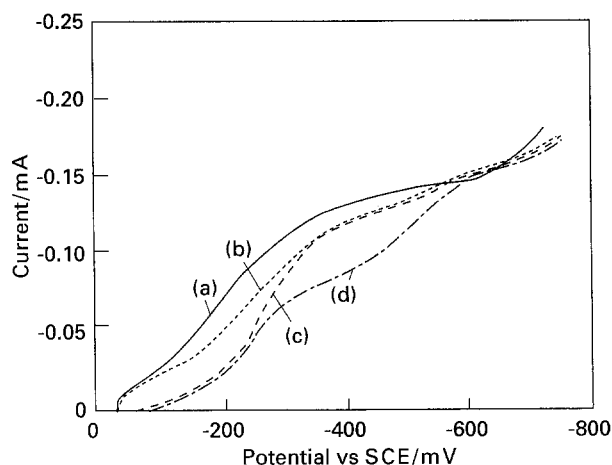


Fig. 10. Current–potential for the reduction of $1 \times 10^{-3} \text{ mol dm}^{-3}$ CuSO_4 in the presence of (a) 0, (b) 1×10^{-6} or 1×10^{-5} , (c) 1×10^{-4} and (d) $1 \times 10^{-3} \text{ mol dm}^{-3}$ DTODSA. WE: Cu RDE, $r = 2 \text{ mm}$, rotation rate: 1250 rpm, RE: SCE and CE: Pt gauze. Potential sweep rate: 10 mV s^{-1} , $T = 293 \text{ K}$.

bonding with the amino nitrogen in the BTA molecule. The films formed by copper and BTA were found to be composed of a near stoichiometric Cu(I)BTA polymer. The thickness of this layer was equivalent to many mono layers of CuBTA monomer. Film growth is believed to occur when the copper ions are transported through the adsorbed BTA film, then an insoluble CuBTA complex is precipitated. The availability of copper ions at the solid/electrolyte interface limits the thickness of the copper film. Polarization studies showed that BTA was an efficient cathodic inhibitor, indicating that the film acts as a physical barrier to electrode reactions.

Pizzini *et al.* [31] have used EXAFS to show that the BTA was only present in the outer atomic layers of the deposit. The inhibiting effect of BTA is believed to be due to the chemisorption of BTA at the copper surface, which produces a film containing Cu(I)–BTA polymeric chains. The co-ordination of the metallic copper shell is reduced by approximately 50% after copper is treated with BTA. The amount of oxygen present at the surface seems to be almost doubled [31]; however, EXAFS cannot clearly distinguish between oxygen and nitrogen back scattered electrons so one of the two shells may more effectively be attributed to the nitrogen in the triazole ring. The Cu–BTA complex forms due to the increased amount of oxygen or nitrogen coordinated to the copper surface. The thickness of the Cu–BTA layer was found to be very small, 1.0–1.5 nm [31].

3.6. Copper deposition in the presence of 4,5-dithiaoctane-1,8-disulphonic acid

Polarization curves for 1×10^{-6} to $1 \times 10^{-3} \text{ mol dm}^{-3}$ DTODSA in $1 \times 10^{-3} \text{ mol dm}^{-3}$ CuSO_4 are shown in Fig. 10. In the absence of additive, a characteristic polarization curve was obtained with the limiting current plateau region occurring at around -380 mV . On addition of 1×10^{-6} to $1 \times 10^{-5} \text{ mol dm}^{-3}$

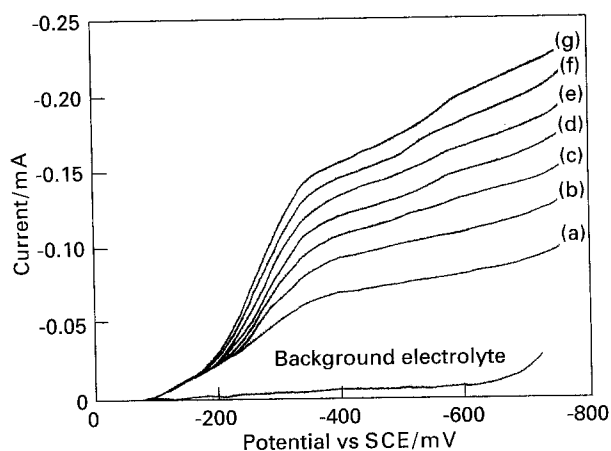


Fig. 11. Current-potential curves for the reduction of $1 \times 10^{-3} \text{ mol dm}^{-3} \text{ CuSO}_4$ in the presence of $1 \times 10^{-4} \text{ mol dm}^{-3}$ DTODSA; background electrolyte $0.5 \text{ mol dm}^{-3} \text{ Na}_2\text{SO}_4$ at pH 2.0 for rotation rates of (a) 250, (b) 500, (c) 750, (d) 1000, (e) 1250, (f) 1500 and (g) 1750 rpm. WE: Cu RDE, $r = 2 \text{ mm}$, RE: SCE and CE: Pt gauze. Potential sweep rate: 10 mV s^{-1} , $T = 293 \text{ K}$.

DTODSA similar curves were obtained but the currents in the charge transfer and mixed control regions were reduced and only at potentials more negative than -580 mV did the curves resemble those obtained for the additive free solution. At concentrations of $1 \times 10^{-3} \text{ mol dm}^{-3}$ DTODSA a new feature centred at -230 mV was observed. This may be due to the presence of copper (i), produced by the formation of a complex with DTODSA. The rest potential became slightly more negative at higher DTODSA levels, values ranging from -46 mV in the absence of additive, to -56 mV with $1 \times 10^{-4} \text{ mol dm}^{-3}$ DTODSA, after which the value remained constant.

Figure 11 shows the limiting currents for a $1 \times 10^{-4} \text{ mol dm}^{-3}$ concentration of DTODSA copper solution. The diffusion coefficient was $6.8 \pm 0.4 \text{ cm}^2 \text{ s}^{-1}$ over the range of additive concentrations investigated. As in the case of TU and BTA additions, the Tafel slope increased from $-120 \pm 3 \text{ mV}$ in the additive free copper solution to a value of $-190 \pm 5 \text{ mV}$ in the presence of 1.1×10^{-6} to $5.5 \times 10^{-4} \text{ mol dm}^{-3}$ DTODSA, as shown in Fig. 12. This value only altered at concentrations of $1.1 \times 10^{-3} \text{ mol dm}^{-3}$ DTODSA where a Tafel slope of $-204 \pm 4 \text{ mV}$ was observed. Similar behaviour was also seen for high concentrations of BTA and TU. A charge transfer coefficient of 0.30 was calculated for a Tafel slope of -190 mV , indicating a more complicated electro-deposition process. There was, however, a significant difference in the exchange current densities for copper deposition from solutions containing DTODSA and those with either TU or BTA. In the presence of $1.1 \times 10^{-3} \text{ mol dm}^{-3}$ DTODSA, a value of $0.16 \pm 0.002 \text{ mA cm}^{-2}$ was obtained for the exchange current density compared to that of $0.0085 \pm 0.0003 \text{ mA cm}^{-2}$ in the additive free solution. This indicates more favourable kinetics for the copper deposition reaction in the presence of DTODSA.

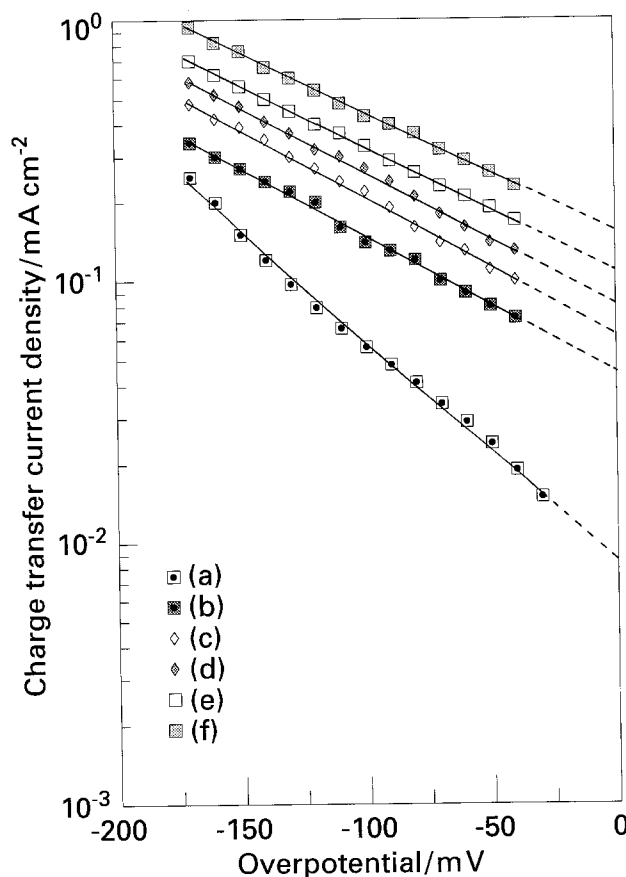
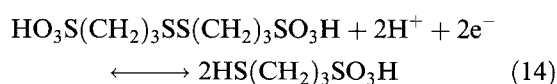


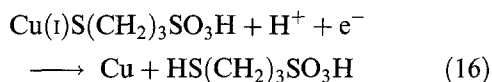
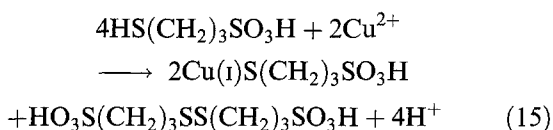
Fig. 12. Tafel extrapolations for $1 \times 10^{-3} \text{ mol dm}^{-3} \text{ CuSO}_4$ in 0.5 mol dm^{-3} nitrogen purged Na_2SO_4 at pH 2.0 in the presence of (a) 0, (b) 1.1×10^{-5} , (c) 5.5×10^{-5} , (d) 1.1×10^{-4} , (e) 5.5×10^{-4} and (f) $1.1 \times 10^{-3} \text{ mol dm}^{-3}$ DS-4. WE: Cu RDE, $r = 2 \text{ mm}$, rotation rate: 1250 rpm, RE: SCE and CE: Pt gauze. Potential sweep rate: 1 mV s^{-1} , $T = 293 \text{ K}$.

3.7. Mechanism of action of 4,5-dithiaoctane-1,8-disulphonic acid

Adsorbed layers of brighteners generally produce inhibition of metal deposition, as illustrated by the results obtained for copper in the presence of TU and BTA. However, in contrast, DTODSA, shows a depolarizing effect [32–35] and mechanisms accounting for this generally involve the formation of surface complexes, containing organic ligands which reduce more rapidly and at more positive potentials than the corresponding aquo complexes, thus lowering the activation energy barrier [32].

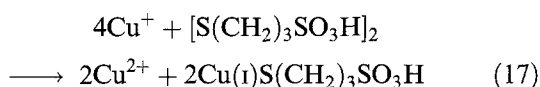
Zukauskaitė *et al.* [32, 33] used potentiodynamic and UV spectroscopic techniques to show that, over the range of potentials used for copper deposition, Cu(I) organo complexes were present and that DTODSA was electroreduced to 3-mercapto-propane-sulphonic acid (MPS), $\text{HS}(\text{CH}_2)_3\text{SO}_3\text{H}$ (see Equation 14). MPS then reduces Cu^{2+} to produce a Cu(I) thiolate complex and DTODSA is regenerated. The DTODSA can again be reduced whilst the Cu(I) complex undergoes reduction to produce copper metal and MPS. A possible reaction mechanism is as follows [32, 33]:



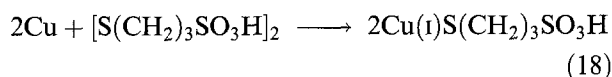


DTODSA is therefore able to participate in repeated oxidation and reduction cycles and depolarization occurs because Cu^{2+} reduction to Cu^+ occurs chemically in reactions involving the additive in contrast to a purely electrochemical Cu^{2+} to Cu^+ electroreduction process.

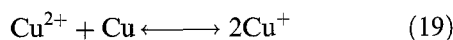
Healy *et al.* [34, 35] suggested an alternative mechanism for the decomposition of DTODSA in electroplating baths. This again involved the formation of a stable Cu(I) complex $\text{Cu(I)}\text{S}(\text{CH}_2)_3\text{SO}_3\text{H}$, however, in this mechanism DTODSA reacts directly with Cu^{2+} ions to form the complex:



The observed reduction of DTODSA is only possible because of the strong interaction of the thiolate ion with the Cu(I). In the absence of complex formation, neither Cu(I) nor Cu(0) are strong enough to reduce DTODSA. In the absence of cupric ions only slow electrodeposition occurs and it is believed that in this case copper metal itself becomes the reducing agent:



Although copper metal is a stronger reducing agent than cupric ions, the decomposition reaction is slower because of the reproporationation reaction.



Healy *et al.* [35] also showed that in the presence of $50 \times 10^{-3} \text{ mol dm}^{-3}$ DTODSA a film formed at the electrode surface attributed to a Cu(I) complex consisting of mainly $\text{Cu(I)}\text{S}(\text{CH}_2)_3\text{SO}_3\text{H}$. This film was formed at potentials less negative than -0.8 V vs Hg/HgSO_4 and at potentials greater than -0.97 V vs Hg/HgSO_4 the film underwent further reduction to copper metal.

When low levels of DTODSA (typically 1 to $2 \times 10^{-6} \text{ mol dm}^{-3}$) were present in solution, the rate of film formation at the electrode surface was negligible. A detailed mechanism of this film formation was not given but the film appears to form readily at sites on the electrode surface where there is a high flux of DTODSA, for example, at the tips of forming dendrites and this leads to the inhibition of the metal deposit at sites of high local current density. The film is removed by cathodic reduction. Passivation of the surface will lead to higher local densities and the resulting shift in potential to more negative values will lead to the reduction of the film to copper.

In this paper an evaluation of the effects of single additives on the electrodeposition of copper from dilute solutions has been carried out. Further studies will involve mixtures of additives and the selective deposition of metals from mixed metal systems. In addition, additives known to affect the mass transport controlled reaction as opposed to charge transfer system studied here will be investigated.

4. Conclusions

The effects of a series of organic additives on the electrodeposition of copper from dilute acidic sulphate solutions have been investigated. These studies show the following effects:

(i) The presence of TU, BTA or DTODSA in copper solutions did not affect the region of mass transport control for copper deposition. However, in the case of TU the limiting current plateau became less well defined.

(ii) The cathodic Tafel slope for additive free copper solutions was $-120 \pm 3 \text{ mV}$, with a charge transfer coefficient of 0.50 and the exchange current density increased with cupric ion concentration.

(iii) In all cases, the Tafel slopes b_C , increased from $-120 \pm 3 \text{ mV}$ for additive free copper solution to -164 ± 4 , -180 ± 2 and $-194 \pm 5 \text{ mV}$ for TU, BTA and DTODSA, respectively. These results correspond to charge transfer coefficients of 0.35 for TU, 0.32 for BTA and 0.30 for DTODSA, assuming a one electron change. The changes in b_C and a_C show that the reaction taking place at the electrode surface no longer involves a simple one electron change.

(iv) In the presence of TU or BTA the exchange current density for copper deposition decreased. In the case of TU there was no correlation between additive concentration and change in exchange current density; whereas, with BTA the exchange current density decreased systematically at higher BTA concentrations. TU and BTA acted as inhibitors for the copper deposition. In the presence of DTODSA, the exchange current density increased at higher DTODSA concentration and this additive is believed to catalyse copper deposition.

References

- [1] F. C. Walsh and G. W. Reade, in 'Environmental orientated electrochemistry' (edited by C. A. C. Sequeira), Elsevier, Amsterdam (1994) pp 3–44.
- [2] D. Pletcher and F. C. Walsh, 'Industrial electrochemistry', 2nd edn, Blackie A & P, Glasgow (1993) p. 333.
- [3] B. Ke, J. J. Hoekstra, B. C. Sissons Jr and D. Trivich, *J. Electrochem. Soc.* **106** (1959) 382–8.
- [4] D. R. Turner and G. R. Johnson, *ibid.* **109** (1962) 798–804.
- [5] D. Pletcher and F. C. Walsh, *op. cit.*, Ref. 2, pp. 403–4.
- [6] M. J. Armstrong and R. H. Muller, *J. Electrochem. Soc.* **138** (1991) 2303–7.
- [7] E. Mattsson and J. O'M. Bockris, *Trans. Faraday Soc.* **55** (1959) 1586–601.
- [8] J. O'M. Bockris and M. Enyo, *ibid.* **58** (1962) 1187–202.
- [9] O. R. Brown and H. R. Thirsk, *Electrochim. Acta* **11** (1965) 383–93.
- [10] U. Bertocci, *Electrochim. Acta* **10** (1965) 1261–77.

- [11] A. De Agostini and E. Schmidt, *Electrochim. Acta* **34** (1989) 1243–8.
- [12] J. R. White, *J. App. Electrochem.* **17** (1987) 977–82.
- [13] I. R. Burrows, J. A. Harrison and J. Thompson, *J. Electroanal. Chem.* **51** (1975) 241–9.
- [14] D. Pletcher, I. Whyte, F. C. Walsh and J. P. Millington, *J. Appl. Electrochem.* **21** (1991) 659–66.
- [15] F. C. Walsh and D. R. Gabe, *ibid.* **13** (1983) 3–22.
- [16] A. J. Arvia, J. C. Bazan and J. S. W. Carrozza, *Electrochim. Acta* **11** (1966) 881–7.
- [17] A. R. Gorden and A. Cole, *J. Phys. Chem.* **40** (1936) 733–7.
- [18] D. Leaist, *Electrochim. Acta* **34** (1989) 651–5.
- [19] T. I. Quickenden and X. Jiang, *ibid.* **29** (1984) 693–700.
- [20] J. P. Healy, D. Pletcher and M. Goodenough, *J. Electroanal. Chem.* **338** (1992) 155–65.
- [21] T. Hurlen, *Acta Chemica Scandinavica* **15** (1961) 630–44.
- [22] C. J. Milora, J. F. Henricksen and W. C. Hahn, *J. Electrochem. Soc.* **120** (1973) 488–92.
- [23] N. Zukauskaitė and A. Malinauskas, *Electrochimica Acta* **24** (1988) 1567–70.
- [24] F. A. Cotton and G. Wilkinson, 'Advanced Inorganic Chemistry', 4th edn, Wiley, Chichester UK (1980) p. 188.
- [25] R. L. Carlin, 'Transition metal chemistry' vol 5, Marcel Dekker, London, New York (1969) p. 142.
- [26] E. E. Farndon, F. C. Walsh and S. A. Campbell, to be published.
- [27] B. S. Shedshadri, *J. Electroanal. Chem. Interf. Electrochem.* **61** (1975) 353–60.
- [28] H. Podsiadly, *Chem. Stosow.* **33** (1989) 91–105.
- [29] A. R. Siedle, R. A. Velapoldia and N. Erickson, *Inorg. Nucl. Chem. Lett.* **15** (1979) 33–6.
- [30] G. W. Poling, *Corr. Sci.* **10** (1970) 359–70.
- [31] S. Pizzini, K. J. Roberts, I. Dring, R. J. Oldman and G. N. Greaves, Conference Proceedings of the Italian Physics Society (1990) pp. 525–28.
- [32] N. Zukauskaitė and A. Malinauskas, *Soviet Metallurgy* **25** (1989) 1362–6.
- [33] *Idem*, *Electrochimica Acta* **24** (1988) 1564–6.
- [34] J. P. Healy, D. Pletcher and M. Goodenough, *J. Electroanal. Chem.* **338** (1992) 167–77.
- [35] *Idem*, *J. Electroanal. Chem.* **338** (1992) 179–87.